Ecotoxicology and Environmental Safety 280 (2024) 116550

Contents lists available at ScienceDirect

Ecotoxicology and Environmental Safety

journal homepage: www.elsevier.com/locate/ecoenv

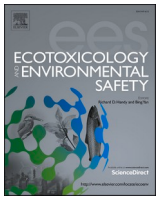

Optimization of desorption parameters using response surface methodology for enhanced recovery of arsenic from spent reclaimable activated carbon: Eco-friendly and sorbent sustainability approach

Jonas Bayuo [a,b,c,*], Mwemezi J. Rwiza [b], Joon Weon Choi [a], Mika Sillanpää [d,e,f,g,h], Kelvin Mark Mtei [b]

[a] Institutes of Green Bio Science and Technology, Seoul National University, Pyeongchang-daero 1447, Gangwon-do, South Korea
[b] School of Materials, Energy, Water, and Environmental Sciences (MEWES), The Nelson Mandela African Institution of Science and Technology (NM-AIST), P.O. Box 447, Arusha, Tanzania
[c] Department of Science Education, School of Science, Mathematics, and Technology Education (SoSMTE), C. K. Tedam University of Technology and Applied Sciences (CKT-UTAS), Postal Box 24, Navrongo, Upper East Region, Navrongo, Ghana
[d] Functional Materials Group, Gulf University for Science and Technology, Mubarak Al-Abdullah, Kuwait 32093, Kuwait
[e] Centre of Research Impact and Outcome, Chitkara University Institute of Engineering and Technology, Chitkara University, Rajpura, Punjab 140401, India
[f] Division of Research & Development, Lovely Professional University, Phagwara, Punjab 144411, India
[g] Department of Chemical Engineering, School of Mining, Metallurgy and Chemical Engineering, University of Johannesburg, P. O. Box 17011, Doornfontein 2028, South Africa
[h] Sustainability Cluster, School of Advanced Engineering, UPES, Bidholi, Dehradun, Uttarakhand 248007, India

ARTICLE INFO

Editor: Dr. G. Liu

Keywords:
Adsorption
Adsorbent
Arsenic
Desorption
Eluent
Optimization

ABSTRACT

Desorption and adsorbent regeneration are imperative factors that are required to be taken into account when designing the adsorption system. From the environmental, economic, and practical points of view, regeneration is necessary for evaluating the efficiency and sustainability of synthesized adsorbents. However, no study has investigated the optimization of arsenic species desorption from spent adsorbents and their regeneration ability for reuse as well as safe disposal. This study aims to investigate the desorption ability of arsenic ions adsorbed on hybrid granular activated carbon and the optimization of the independent factors influencing the efficient recovery of arsenic species from the spent activated carbon using central composite design of the response surface methodology. The activated carbon before the sorption process and after the adsorption-desorption of arsenic ions have been characterized using SEM-EDX, FTIR, and TEM. The study found that all the investigated independent desorption variables greatly influence the retrievability of arsenic ions from the spent activated carbon. Using the desirability function for the optimization of the independent factors as a function of desorption efficiency, the optimum experimental conditions were solution pH of 2.00, eluent concentration of 0.10 M, and temperature of 26.63 °C, which gave maximum arsenic ions recovery efficiency of 91 %. The validation of the quadratic model using laboratory confirmatory experiments gave an optimum arsenic ions desorption efficiency of 97 %. Therefore, the study reveals that the application of the central composite design of the response surface methodology led to the development of an accurate and valid quadratic model, which was utilized in the enhanced optimization of arsenic ions recovery from the spent reclaimable activated carbon. More so, the desorption isotherm and kinetic data of arsenic were well correlated with the Langmuir and the pseudo-second-order models, while the thermodynamics studies indicated that arsenic ions desorption process was feasible, endothermic, and spontaneous.

* Corresponding author at: School of Materials, Energy, Water, and Environmental Sciences (MEWES), The Nelson Mandela African Institution of Science and Technology (NM-AIST), P.O. Box 447, Arusha, Tanzania
E-mail addresses: jbayuo@cktutas.edu.gh, bayuoj@nm-aist.ac.tz (J. Bayuo).

https://doi.org/10.1016/j.ecoenv.2024.116550
Received 25 April 2024; Received in revised form 31 May 2024; Accepted 3 June 2024
Available online 5 June 2024

1. Introduction

Several factors including its harmful effects on the natural environment and the sustainable growth of humanity, arsenic-based water pollution is a worldwide problem (Saleh et al., 2021). According to recent studies, several essential organs, including the lungs, skin, liver, bladder, and kidneys may experience impairment due to the consumption of arsenic-contaminated water (Bi et al., 2020). The presence of arsenic species in the ecosystem requires more attention due to its high solubility in aqueous systems as well as its toxicity and sequestration challenges (Deng et al., 2019). Therefore, efforts have been made to remove arsenic species from wastewater resulting from different industries including mining, refinery, tannery, fertilizers, electroplating, dyes, and textiles using traditional technologies including reverse osmosis, solvent extraction, membrane filtration, oxidation, ion exchange, and chemical precipitation (Priyadarshanee and Das, 2021; Kocadagistan and Oksuz, 2022). Even so, there are many drawbacks to these purification technologies, including the production of hazardous secondary chemical sludge, insufficient reduction of metal ions, limited performance, as well as substantial energy and reagents consumption (Ezeonuegbu et al., 2021; Tokay and Akpınar, 2021; Bayuo et al., 2022).

Hence, new cost-effective, safe, and economical water and wastewater treatment methods are required to overcome the challenges of these conventional methods. In comparison to the traditional treatment systems, the adsorption technique is adaptable in both design and operation, and it typically offers high effectiveness in decontaminating water pollutants. Furthermore, the dynamic nature of the adsorption process enabling adsorbent recycling and reusability of the spent adsorbent is one of its key benefits (Hua et al., 2012; Jadidi et al., 2017; Bayuo et al., 2023a, 2023b). Desorption and adsorbent recycling are the main imperative variables for designing the desorption process, which is described by the recovery of the bounded ions and the regeneration of the spent sorbent material (Hamza et al., 2022). Undoubtedly, one of the sustainability and regenerative elements that demonstrate the adsorption approach is environmentally friendly is the ability to recover adsorbed heavy metal ions and reuse the previously utilized sorbent material. In reality, when the used adsorbents are not regenerated and properly disposed of will lead to more environmental pollution.

Additionally, the storage and disposal of used adsorbents may result in fires, explosions, and foul odors (Vakili et al., 2019). The reusability of the sorbent material is determined by its adsorption and desorption characteristics and as a result it is crucial that the adsorbent is simple to renew and the desorbing agent is efficient, affordable, non-polluting, and not destructive to the surface chemistry of the adsorbent (Kołodyńska et al., 2017; Taşdemir et al., 2021). The extraction of the metal ions from the used adsorbent can be accomplished with desorption eluents such as acid or alkaline solutions or deionized water when the mechanism of adsorption of the metal ions by the adsorbent is mainly due to ion exchange or chemical bonding (Staroń et al., 2021). Hence, desorption is performed to extract as many adsorbed metal ions from the used adsorbent as possible as well as to potentially regenerate and reuse the adsorbent. Due to the importance of renewability in commercial adsorbent and industrial applications, the ideal sorbent material is expected not only to have a greater capacity for the adsorption of heavy metals but also to have improved recovery efficiency, as this would greatly improve reusability and lower the overall cost in producing the adsorbent (Alimohammady et al., 2017; Karapinar et al., 2021).

Due to the high cost of production and disposal, greater focus has been placed on the regeneration and reuse of the spent adsorbents (Vakili et al., 2019). Several studies have found that for any large-scale application of adsorbents derived from biomass for heavy metals remediation from aqueous systems, the regeneration, and reuse of used adsorbents are crucial (Ghangale et al., 2019; Touihri et al., 2021). The desorption behavior of heavy metal ions adsorbed on agricultural biomass-derived activated carbon, which is thought to be crucial to understanding the resiliency of the adsorption process, has, however, received very little research attention (Li et al., 2018; Xie et al., 2018; Lu et al., 2019; Zou et al., 2019; Gan et al., 2020). In addition, there is no study on the optimization of desorption parameters influencing the retrievability of absorbed adsorbate molecules from the adsorbent and the regeneration of the spent adsorbent for subsequent use.

Therefore, for the first time, the present study investigates the optimization of desorption variables using a statistical experimental design for the effective retrieval of arsenic ions from the previously spent hybrid granular activated carbon. Three independent desorption variables such as eluent pH and concentration as well as desorption temperature were evaluated using a central composite design of the response surface methodology to establish the optimal operating conditions for effective and high arsenic ions desorption from the spent activated carbon for the purpose of reusability and proper disposal of the exhausted sorbent material. The central composite design of the response surface methodology is a statistical tool that is applied in industrial process optimization using large experimental data obtained from a minimum number of designed experiments.

2. Materials and methods

2.1. Activated carbon preparation and characterization

In this study, the proficient recovery of arsenic ions from spent hybrid granular activated carbon (adsorbent) and the optimization of desorption variables influencing the process were explored. The hybrid granular activated carbon was synthesized from maize plant biomass in accordance with the procedures outlined previously by Bayuo et al. (2023). Maize plant residues are carbon-rich in nature and possess lignocellulose constituents containing several surface functional groups, which are capable of binding heavy metals from wastewater. In Africa and other parts of the world, huge numbers of maize residues are produced throughout the season posing environmental nuisance and disposal issues. Hence, the production of hybrid granular activated carbon from the maize plant biomass provides a cost-effective technological solution to arsenic pollution and waste disposal challenges in the environment. The hybrid granular activated carbon before the sorption process as well as after the adsorption and desorption of arsenic ions have been characterized using Scanning Electron Microscopy (SEM) coupled with Energy Dispersive X-ray (EDX) analysis, Fourier Transform Infrared Spectrometer (FTIR), and Transmission Electron Microscopy (TEM).

All of the laboratory reagents and chemicals acquired and utilized by this research were of analytical quality. Such as hydrochloric acid (HCl, 37 %), sodium hydroxide (NaOH, 97 %)), phosphoric acid (H_3PO_4, 85 %), nitric acid (HNO_3, 68 %), Ethylenediaminetetraacetic acid (EDTA, 99 %), deionized and distilled water.

2.2. Industrial wastewater sampling and adsorption studies

Real wastewater from a textile-based industry was collected, processed, handled, and analyzed in accordance with the guidelines for wastewater and water examination (Gilcreas, 1967). The collected wastewater was kept in plastic bottles and treated with HNO_3 to acidify them to a pH of less than 2.0 before being transferred to the laboratory for testing within 4.0 h at a temperature of 4.0 °C. At the laboratory, the wastewater was characterized by an atomic absorption spectrophotometer using the standard protocols in APHA (Gilcreas, 1967) to detect the possible heavy metals/metalloids and their concentrations in the wastewater. Subsequently, the wastewater was put through an adsorption test by the activated carbon utilizing a batch method, whereby 100 mL of the wastewater was transferred in 250 mL Erlenmeyer flasks, and 0.5 g/L activated carbon dosage was added. The batch experiments were carried out with 90.0 μm activated carbon particle size, a pH of 6.0, and an agitation period of 60.0 min. Using a flask rotary shaker, the sample mixtures were shaken at 120.0 rpm at a room temperature of

20.0 ℃. The sample mixtures were then centrifuged and filtered with 0.42 μm Whatman filtering paper following the shaking period. The quantity of arsenic species adsorbed on the activated carbon was determined by using Eq. (1) by measuring the total arsenic in the supernatant via atomic absorption spectrophotometer at a wavelength of 193.70 nm (Ciopec et al., 2021).

$$q_t = \left(\frac{C_0 - C_t}{W}\right) \times V \quad (1)$$

where C_0 is the baseline concentration of arsenic before the sorption process, C_t is the amount of arsenic in the aqueous phase at a particular adsorption time, q_t is the arsenic ions uptake capacity at a precise time, W is the mass (g) of activated carbon, and V is the solution volume (L).

2.3. Experimental design for desorption process modeling and optimization

The central composite design of the response surface methodology was used to investigate the interactive effects of desorption factors such as solution pH and eluent concentration as well as desorption temperature. In the past few years, the central composite design of the response surface methodology has emerged as the top multivariate statistical tool for heavy metals adsorption process optimization (Dulla et al., 2020; Bangaraiah et al., 2021; Corral-Bobadilla et al., 2021; Khoshraftar et al., 2023). The central composite design of the response surface methodology optimization studies is highly helpful in lowering operation time and cost. It is also asserted that the results acquired through the central composite design of the response surface methodology are statistically acceptable in addition to the decrease in experimental runs (Biswas et al., 2019; Afraz et al., 2020). The experimental data of the response (Y) could be analyzed by the second-order polynomial equation as a function of independent desorption variables (Fawzy, 2020; Afolabi et al., 2021):

$$Y = b_0 + \sum_{i=1}^{n} b_i X_i + \sum_{i=1}^{n} b_{ii} {X_i}^2 + \sum_{i=1}^{n-1} \sum_{j=i+1}^{n} b_{ij} X_i X_j + \varepsilon \quad (2)$$

where Y is the predicted response factor, b_0 is the constant coefficient, b_i is the linear coefficient, b_{ij} is the interaction coefficient, b_{ii} is the quadratic coefficient, X_i and X_j are the coded values of the factors, and ε is the error function (Biswas et al., 2020).

In the current study, three most influencing variables and their levels were selected from the one-factor-at-a-time batch experiments as described in Text S1 to model and optimize the desorption efficiency of arsenic ions loaded on the activated carbon and the regeneration of the spent activated carbon for further reuse. The number of experimental runs needed for designing, modeling, and optimizing the three independent desorption variables was 20 as determined by Eq. (2) (Kushwaha and Dutta, 2017; Brahmi et al., 2019).

$$N = 2^k + 2k + C_0 \quad (3)$$

where N is the total number of experiments to be performed, k is the number of independent desorption process factors, and C_0 is the number of center points.

2.4. Experimental design by central composite design

To optimize the desorption process, batch experiments were statistically designed by the central composite design of the response surface methodology in the Design Expert Software Version 13, Stat-Ease using three independent desorption factors, and each factor was set at three levels (−1.00, 0.00, +1.00) as listed in Table S1. The batch desorption experiments were carried out by applying the appropriate dosage of the spent activated carbon into a series of Erlenmeyer flasks holding 100 mL of the best recovery eluent (HCl), with varying concentrations provided by the central composite design of the response surface methodology as displayed in Table S2. By utilizing 0.1 M solutions of HCl or NaOH, the appropriate eluent pH was achieved. Both the pH of the eluent and temperature were also adjusted according to the central composite design of the response surface methodology matrix using a pH meter and digital water bath, respectively. Similarly, after each desorption test, the amount of arsenic ions recovered was determined by the atomic absorption spectrophotometer.

3. Results and discussion

3.1. Activated carbon characterization

The scanning electron micrograph of the activated carbon before the sorption process of arsenic ions is presented in Fig. 1(a).

The SEM micrographs were observed to appear more porous and rough with uneven and irregular large cavities which could facilitate the interaction between the arsenic ions and the activated carbon surface leading to efficient decontamination of the arsenic ions from the industrial wastewater. The presence of the mesopores in the activated carbon is due to the impregnation and chemical activation of carbon precursor with H_3PO_4. Fig. 1(b) shows the scanning electron micrograph of the activated carbon after the adsorption of arsenic ions from the wastewater. The disappearance of the mesopores from the activated carbon surface demonstrated the efficient adsorption of arsenic ions by the adsorbent. Also, Fig. 1(c) depicts the scanning electron micrograph of the spent activated carbon after the desorption of the arsenic species from its surface using HCl as the best elution agent. It is observed in Fig. 1(c) that there is a re-emergence of the mesopores that were occupied by the arsenic ions in Fig. 1(b) indicating the successful desorption of the arsenic ions. Hence, the spent activated carbon can be regenerated and reused for further sorption studies.

The elemental composition of the activated carbon determined by the energy dispersive x-ray before the sorption process of arsenic ions from the wastewater is displayed in Fig. 2(a). The elements found in the activated carbon with the highest percentage weight composition (wt%) include carbon (C), oxygen (O), phosphorus (P), and silicon (Si). After the application of the activated carbon for the adsorptive sequestration of arsenic ions from the wastewater, it was observed that the elemental arsenic was present in the energy dispersive x-ray results as shown in Fig. 1(b). This observation showed that the adsorption of arsenic ions on the activated carbon was successful. Fig. 2(c) also represents the energy dispersive x-ray image after the desorption process, in which the elemental arsenic that was present in the micrograph presented in Fig. 2 (b) disappeared suggesting complete desorption of the arsenic ions on the spent activated carbon surface using the HCl as a stripping agent. The effective retrieval of the adsorbed arsenic ions from the used activated carbon is indicative of the renewability and reusability of the as-prepared adsorbent.

The transmission electron micrographs of the untreated activated carbon with the arsenic ions are presented in Fig. 3(a), which revealed that the activated carbon is transparent and highly porous. The highly porous microstructure could increase the surface area of the activated carbon and promote the adsorption of arsenic ions from the wastewater.

In Fig. 3(b), it was found that after the sequestration of arsenic ions from the wastewater, the pores that were observed in Fig. 3(a) were filled up and the presence of the tiny spherical shapes on the activated carbon surface confirmed the proficient adsorption of arsenic ions. The tiny spherical shapes that were purported to represent the arsenic ions adsorbed on the activated carbon surface were found to disappear as shown in Fig. 3(c) indicating that the desorption of the arsenic ions from the spent activated carbon was achieved effectively. Due to the fact that the adsorbed arsenic ions could be recovered completely from the spent activated carbon, this novel adsorbent is promising, regenerable, and can be utilized repeatedly for the remediation of arsenic from wastewater.

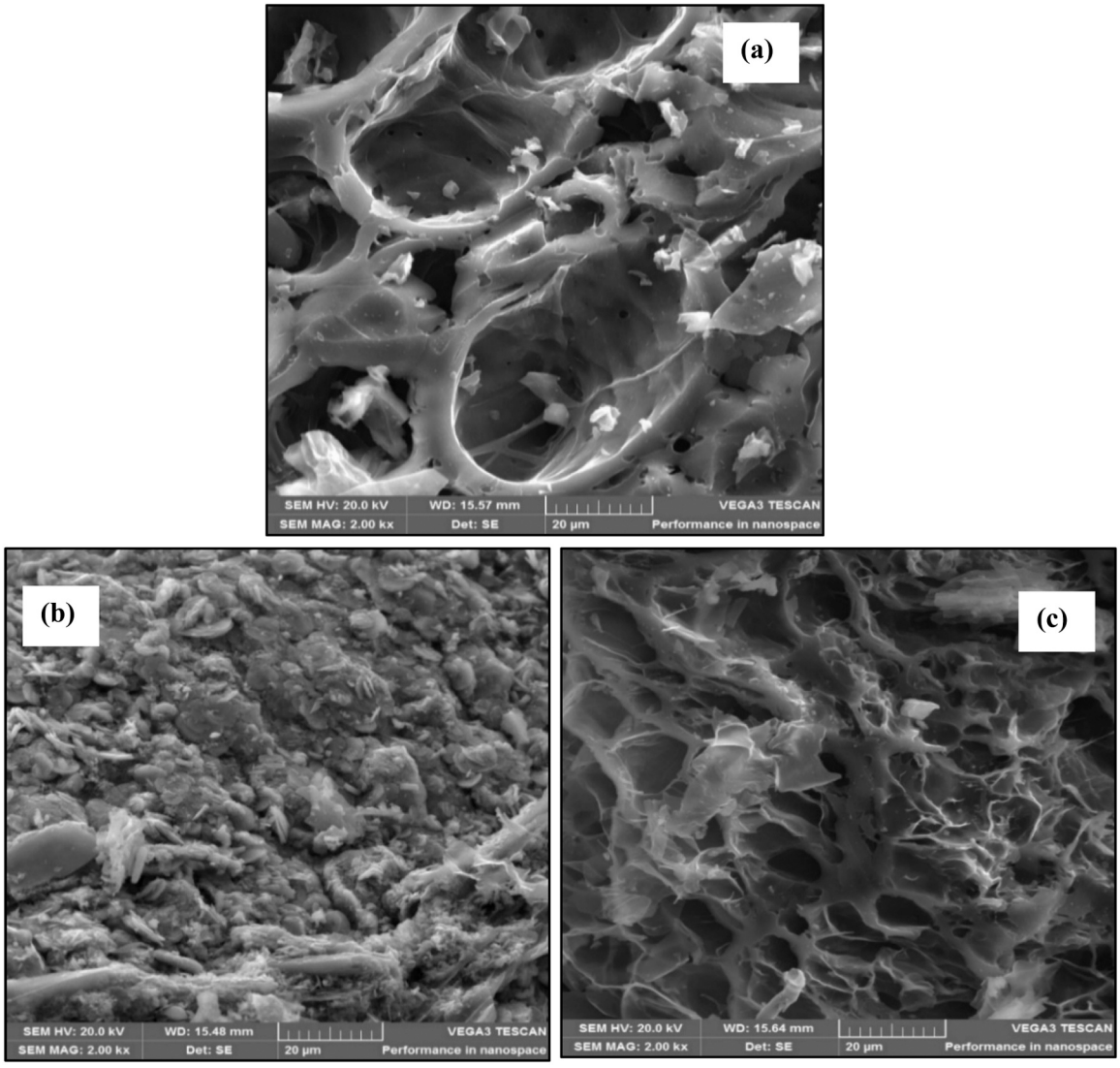

Fig. 1. SEM images of the activated carbon before the sorption process **(a)**, after the adsorption **(b),** and desorption of As ions **(c)**.

The major functional groups found on the activated carbon before the sorption process include hydroxyl (O-H), amino (N–H), and carbonyl (C═O) groups as shown in Fig. 4(a), and they played a crucial function in the uptake of arsenic ions from the wastewater. After the adsorptive sequestration and desorption of the arsenic ions as presented in Fig. 4(b and c), respectively, it was observed that there were shifting and disappearance of wavenumbers of some of the functional groups suggesting that these surface functional groups were accountable for the adsorption-desorption of the arsenic ions. The mechanism of adsorption and desorption of the arsenic ions might be because of the complexation with surface functional groups, ion exchange, and the $\pi-\pi$ interactions with the aromatic complexes on the activated carbon surface.

More importantly, it was observed that after the adsorption and desorption of arsenic species, the FTIR spectra [Fig. (b) and (c), respectively] nearly coincided with the spectrum of the original activated carbon before the beginning of the sorption process [Fig. (a)]. This showed that the microstructure and chemical properties of the activated carbon stayed mostly steady during the process of arsenic ions adsorption and desorption indicating the renewability of the activated carbon for further use.

3.2. *Industrial wastewater characterization and sorption studies*

The physiochemical characterization of the textile wastewater showed that the heavy metals found in the wastewater comprise chromium (VI), arsenic (As), cadmium (Cd), mercury (Hg), lead (Pb), and iron (Fe), in which arsenic concentration was discovered to be far higher than the World Health Organization's approved upper limit (Joseph et al., 2019). The amount of arsenic found in the wastewater was 0.8805 mg/L and after subjecting the wastewater to an adsorption test using 0.50 g/L of the activated carbon in batch mode, the average quantity of arsenic ions adsorbed on the activated carbon was 0.8726 mg/L. This showed that the as-prepared activated carbon is an efficient sorbent material in the removal of arsenic ions from industrial wastewater.

The spent activated carbon was then pretreated by drying in an oven at 105.0 ℃ to a constant mass and utilized in the desorption studies to test the recoverability of the arsenic ions and regeneration of the used activated carbon for the purpose of reusability and proper disposal of the exhausted secondary waste. Five different desorption eluents including de-ionized H_2O, 0.1 M concentration of EDTA, HCl, HNO_3, and H_2SO_4 were tested for stripping off the adsorbed arsenic ions from the spent activated carbon and in testing its reusability and safe disposal. Figure S1 displays the results of the various desorption eluents tested for

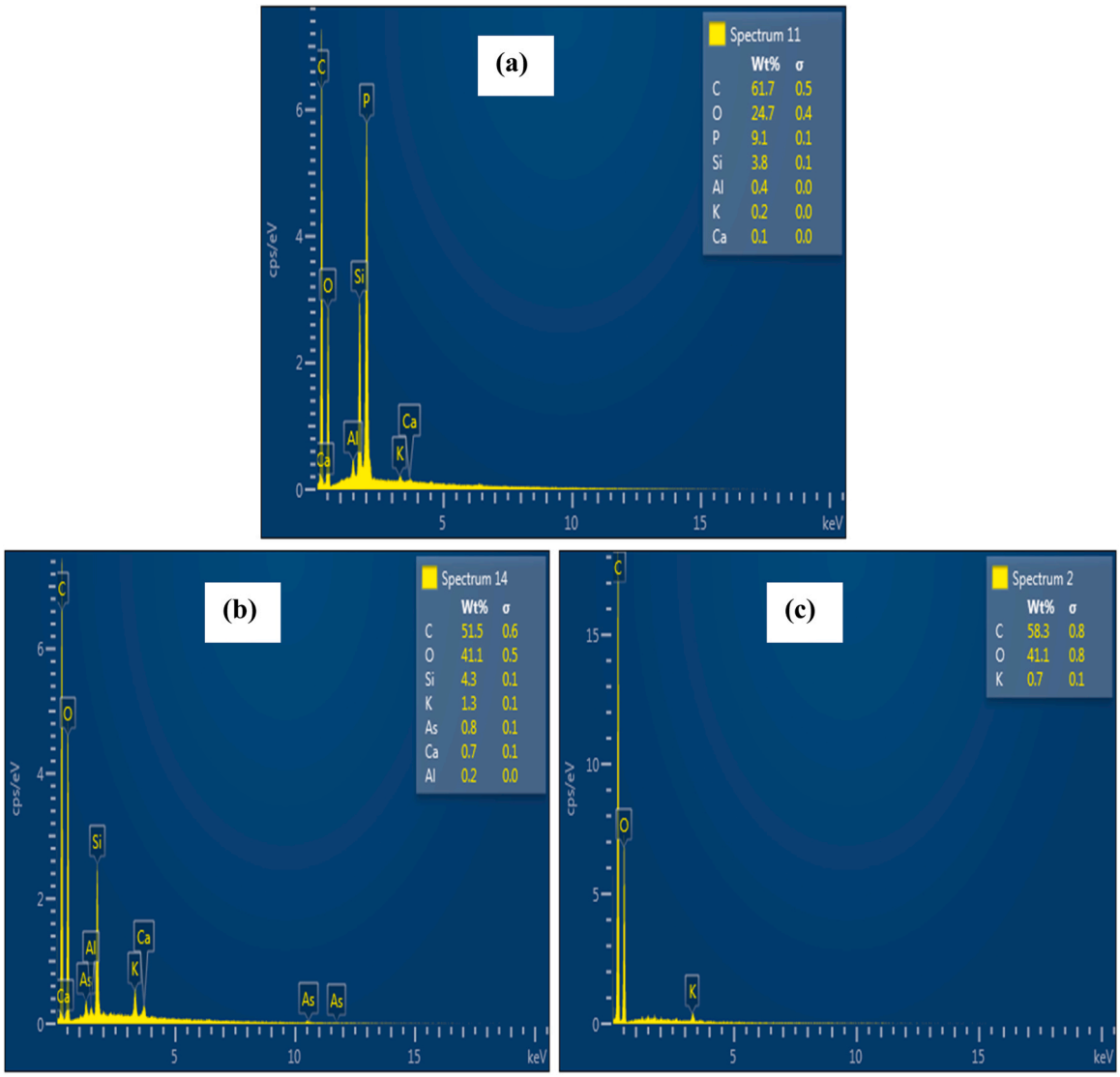

Fig. 2. EDX images of the activated carbon before the sorption process **(a)**, after the adsorption **(b)**, and desorption of As ions **(c)**.

the effective recovery of arsenic ions from the spent activated carbon. A 0.1 M HCl acid solution was found to have the highest arsenic ions recovery of 96.57 %. Similar results were obtained by Mladin et al. (2022) where 5 % HCl was effective in the desorption of about 93 % of As(III) adsorbed on silica-iron oxide nanocomposite. The desorption capability of the various eluents was found to follow the trend: HCl > HNO_3 > EDTA > H_2SO_4 > De-ionized H_2O. The ineffective desorption eluent was de-ionized water with a recovery rate of 12.42 % for arsenic ions. The high desorption rates attained by the HCl indicated that the hydrogen ions undoubtedly play a significant role in the desorption of arsenic ions from the used activated carbon (Zhang et al., 2019). The successful desorption of the arsenic ions from the surface of the activated carbon by HCl suggested an ion exchange mechanism (Bayuo et al., 2020; Bayuo et al., 2023). Therefore, the suitability of using HCl as the best eluent for arsenic ions desorption from the used activated carbon was further tested at varying concentrations.

The results of the effect of the independent variables on the desorption ability of arsenic ions from the spent activated carbon are detailed in Text S2 and shown in Figure S2. These three desorption variables, comprising solution pH, eluent concentration, and temperature were found to significantly influence the desorption efficiency (%) of arsenic ions loaded on the activated carbon and the regeneration of the spent activated carbon for further reuse. Therefore, the central composite design of the response surface methodology was adopted to enhance the desorption rate of arsenic ions from the spent activated carbon as a function of these desorption process factors.

3.3. *Quadratic model development and analysis of variance*

The central composite design of the response surface methodology was used to explore the desorption characteristics of arsenic species loaded on the activated carbon and the optimization of the selected independent variables on the retrieval efficiency of arsenic species from the used activated carbon using HCl as a suitable elution agent. The desorption tests were performed following the experimental layout presented in Table S2, which was statistically designed by the central composite design of the response surface methodology.

The experimental data (Table S3) attained following the experimental design were analyzed using the central composite design of the response surface methodology and a quadratic model equation correlating the independent and the response variables was suggested and selected for the prediction of the response. The accuracy and fit statistics of the developed quadratic model expressed in Eq. (3) are summarized in Table 1.

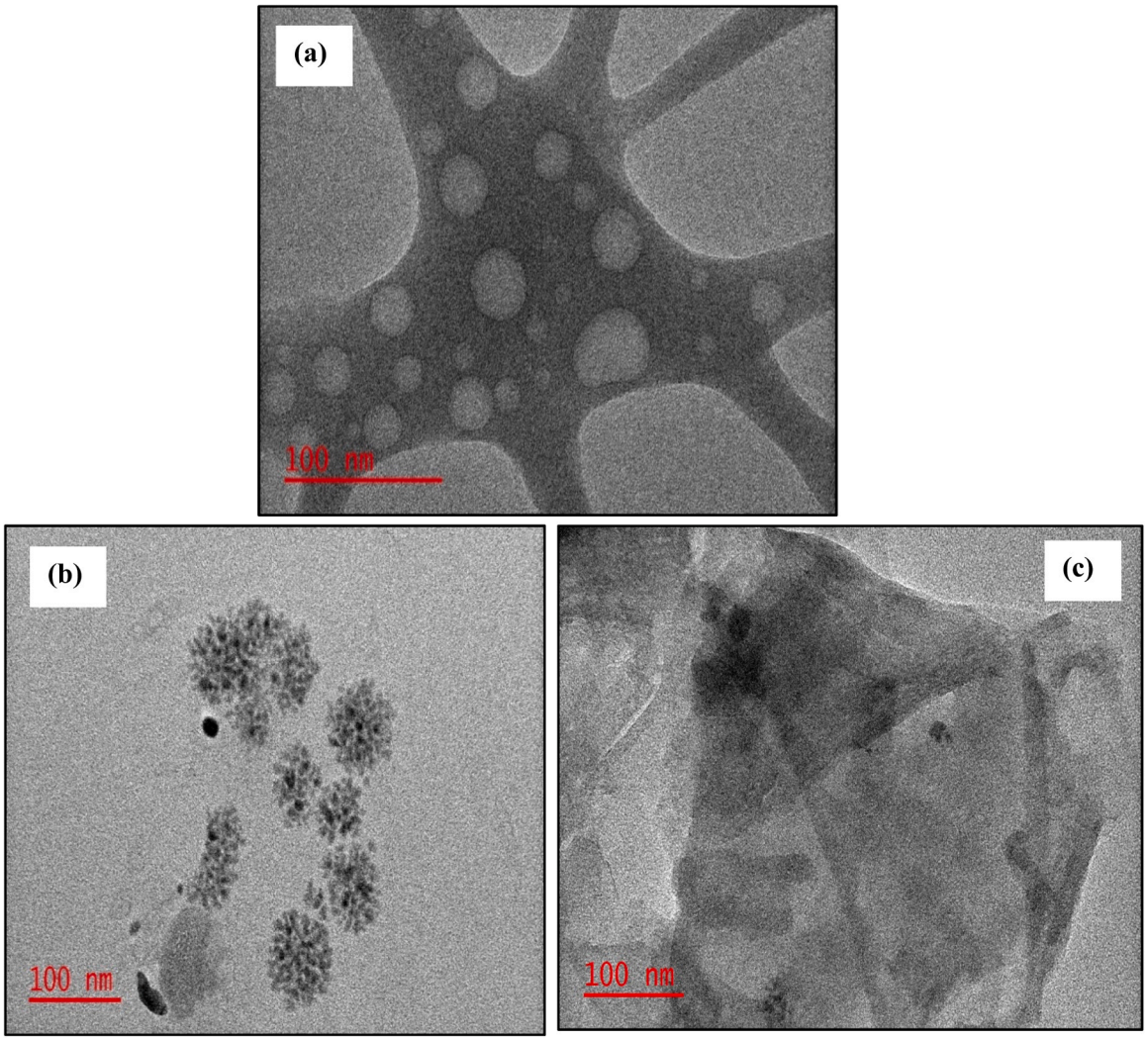

Fig. 3. TEM images of the activated carbon before the sorption process **(a)**, after the adsorption **(b),** and desorption of As ions **(c)**.

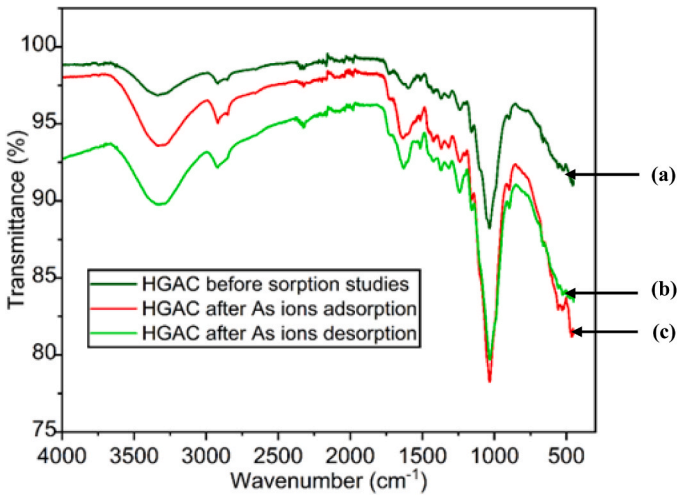

Fig. 4. FTIR spectra of the activated carbon before the sorption process **(a)**, after the adsorption **(b)** and desorption **(c)** of As ions.

$$Y = +71.74 - 4.79A - 0.64B + 5.55C + 4.05AB + 0.88AC + 4.53BC + 5.85A^2 + 3.56B^2 - 7.03C^2 \quad (4)$$

Table 1 illustrates the fit statistics of the quadratic model developed for arsenic ions desorption efficiency from the spent activated carbon. The correlation coefficients such as R-squared (R^2), adjusted $R^{2,}$ and predicted R^2 values of 0.9555, 0.9111, and 0.7866, respectively were observed to be close to unity. A closer correlation coefficient (R^2) to 1.0 indicated a greater fitness and better prediction of the response by the quadratic model (Hadiani et al., 2019; El-Ahmady El-Naggar et al., 2020). Furthermore, there is a discrepancy of less than 0.2 between the adjusted R^2 of 0.9111 and the predicted R^2 of 0.7866, which is indicative of good conformity of the model to the experimental data (Parmar et al., 2020; Ünügül and Nigiz, 2022). Similarly, the lack of fit P-value of 0.6530 demonstrated that the quadratic model's lack of fit is not significant proving that the developed model is accurate and suitable for fitting the experimental data (Mondal et al., 2019; Hannachi and Hafidh, 2020).

The analysis of variance was applied to determine the suitability and reliability of the developed quadratic model. The analysis of variance tests such as P-value, degree of freedom, F-value, and the sum of squares for each factor as shown in Table 2 are applied in examining the adequacy of the selected model. The interactive influence of the F-value is well-recognized when the P-value is less than 0.05 implying model

Table 1
Quadratic model fit statistics for arsenic ions desorption efficiency.

Source	Sequential P-value	Lack of Fit P-value	Adjusted R^2	Predicted R^2	R^2	Std. Dev.	
Linear	0.1739	0.0173	0.1298	-0.5685	0.2748	11.41	
2FI	0.5542	0.0138	0.0799	-0.4212	0.3866	11.74	
Quadratic	< 0.0001	0.6530	0.9111	0.7866	0.9555	3.65	Suggested
Cubic	0.6925	0.3480	0.8905	-4.3467	0.9696	4.05	Aliased

Table 2
Analysis of variance for desorption efficiency quadratic model.

Source	Sum of Squares	df	Mean Square	F-value	P-value	
Block	1283.28	1	1283.28			
Model	2575.24	9	286.14	21.49	< 0.0001	Significant
A-pH of solution	313.69	1	313.69	23.56	0.0009	
B-Eluent concentration	5.54	1	5.54	0.4161	0.5350	
C-Desorption temperature	421.38	1	421.38	31.64	0.0003	
AB	130.98	1	130.98	9.84	0.0120	
AC	6.25	1	6.25	0.4692	0.5106	
BC	164.08	1	164.08	12.32	0.0066	
A^2	493.10	1	493.10	37.03	0.0002	
B^2	182.03	1	182.03	13.67	0.0049	
C^2	711.65	1	711.65	53.44	< 0.0001	
Lack of Fit	55.91	5	11.18	0.6997	0.6530	Not significant
C.V.%	4.87					
Adeq Precision	21.31					

adequacy (Gomravi et al., 2021).

Table 2 showed that the P-value of the quadratic model is less than 0.0001 with a high F-value of 21.49 indicating the accuracy of the model (Bhateria and Dhaka, 2019; Lyonga et al., 2021; Mushtaq et al., 2023). Likewise, the non-significant lack of fit revealed the conformity of the quadratic model to the experimental data (Kusrini et al., 2019; Liu et al., 2021). Also, the model terms are statistically significant when the P-value is lower than 0.05, and the model terms are insignificant when the P-value is more than 0.10 (Liu et al., 2019). While A, C, AB, BC, A^2, B^2, and C^2 were found as the significant model terms with $P < 0.05$, the insignificant model terms were B and AC with $P > 0.05$. The fewer the insignificant model terms, the more accuracy the quadratic model is and model reduction is not require to improve the conformity of the model with the experimental data. According to the F-values, the magnitude of the interactive effects exhibited by the significant model terms on the desorption efficiency of arsenic ions from the spent activated carbon is in the sequence of: $C^2 > A^2 > C > A > B^2 > BC > AB$. Besides, the coefficient of variance (C.V.%) value of 4.87 was found to be lower than 10 implying that the quadratic model is reliable and could be applied in the prediction of simlilar data in the future (Khoshraftar et al., 2023). It has been found that the higher the C.V.% value, the lower the quadratic model's reliability (Mahmood et al., 2017; Fawzy et al., 2022). Additionally, the adequate precision of 21.31, which measures the signal-to-noise ratio was found to be far higher than 4.0 demonstrating adequate signal and the model suitability in navigating the design space (Chen et al., 2020).

In Eq. (4), the coefficients of the model terms play a substantial role in the optimization of the desorption process. While the model terms with negative coefficients exhibited antagonistic effects on the desorption efficiency of arsenic ions from the spent activated carbon, the model terms with positive coefficients revealed synergistic effects and promoted the desorption process optimization (Bai and Venkateswarlu,

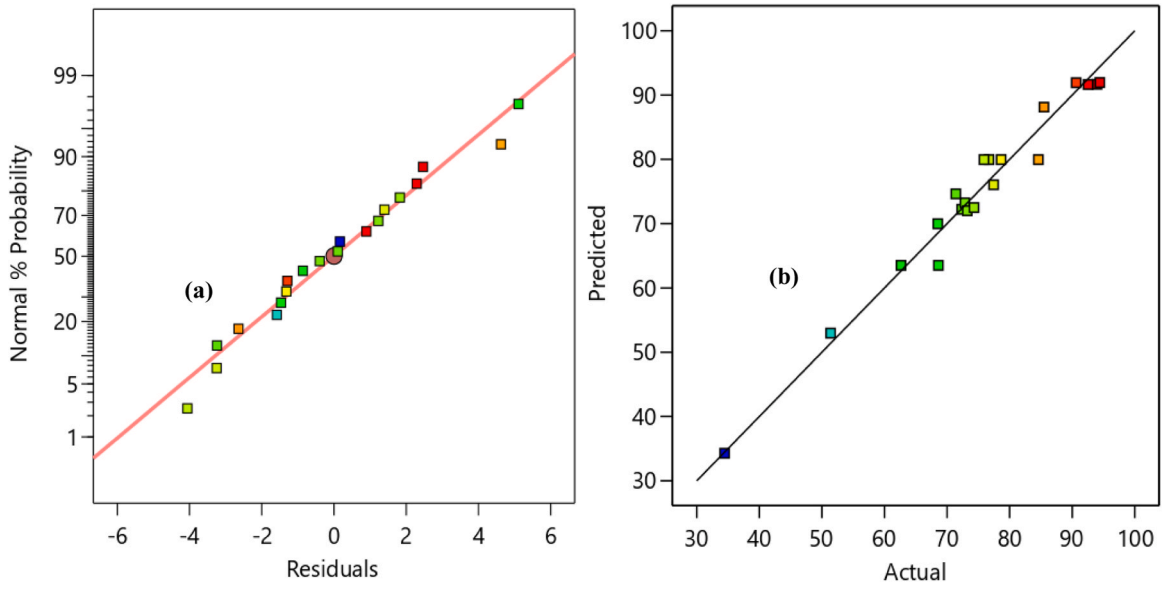

Fig. 5. Normal % probability versus residual values (a) and predicted versus actual values (b) of arsenic desorption efficiency using spent activated carbon.

2019; Brahmi et al., 2019; John et al., 2019). Therefore, the model terms that have synergistic effects on the optimization of the desorption process are C, AB, AC, BC, A^2, and B^2 whereas the antagonistic model terms were found to be A, B, and C^2.

In addition to the analysis of variance, diagnostic tests were carried out to verify the suitability of the selected quadratic model. It can be concluded from the residual analysis that the developed quadratic model for the efficient desorption of arsenic ions on the spent activated carbon is accurate and suitable for the response prediction. In Fig. 5(a), all the residual values were observed to follow a normal distribution, and almost all the residuals were aligned closely along the diagonal line indicating the good fitness of the actual data to the selected quadratic model (Yuan et al., 2019; Cheng et al., 2021). The predicted values by the quadratic model and actual (experimental) values were compared by plotting the predicted against the actual values as shown in Fig. 5(b). Fig. 5(b) showed that all the data points were oriented along and close to the diagonal line signifying minimal variability between the predicted and the experimental values (Liang and Shen, 2022). Several studies found that the smaller the residuals between the actual and predicted values, the more accuracy the predicted values are attained by the quadratic model (Sadhukhan et al., 2016; Biswas et al., 2020).

Table S4 summarizes the actual and predicted values with minimum residuals and the leverage values were found to be less than one, which demonstrates the quadratic model accuracy in predicting the response (Bhateria and Dhaka, 2019). Besides, the interactive effect among the independent desorption factors as a function of desorption efficiency was assessed as detailed in Text S3 using 3-D response surface and contour plots displayed in Fig. S3, Fig. S4, and Fig. S5, respectively. It was found that all the investigated independent desorption variables greatly influence the retrievability of arsenic ions from the spent activated carbon.

3.4. Desorption process optimization and quadratic model validity

The desirability function was employed to determine the ideal experimental operating conditions for which effective and highest recovery of arsenic ions from the spent activated carbon could be attained. The constraints set for the numerical optimization are summarized in Table S5, in which all the independent desorption factors were kept in range and the response variable was set as maximize. Using the constraints set for the optimization process and by applying the central composite design of the response surface methodology, the best operating condition for efficient desorption of arsenic ions from the spent activated was found at a solution pH of 2.0, eluent concentration of 0.1 M, and desorption temperature of 22.63 ℃ after seeking 20 solutions as summarized in Table S6. At this ideal experimental condition, arsenic ions recovery efficiency of 90.62 % with a combined desirability of 0.937 and desirability of 1.00 for each independent factor as presented in Fig. S6 and Fig. S7, respectively.

To validate the quadratic model developed for the desorption ability of arsenic ions from the spent activated carbon, laboratory confirmatory experiments were conducted. Table S7 shows the data mean of the five confirmatory experimental runs performed at a two-sided 95 % confidence level using the best operating conditions achieved during the efficient recovery of arsenic ions on the used activated carbon. The confirmatory experimental results showed that at the optimal conditions suggested in Table S6 (Number 1), the optimum recovery efficiency of 96.75 % was attained. The obtained optimum desorption efficiency from the laboratory experiments is found to be between the 95 % prediction interval of 84.41–96.83 % Therefore, there exists a good conformity between the confirmatory experimental and the predicted results with standard error prediction (SE Pred) of 2.74 indicating that the developed quadratic model is valid and could be used in predicting future cases.

3.5. Desorption modeling and thermodynamic studies

The desorption isothermal data of arsenic fitted into the Langmuir and the Freundlich isotherm models described in Text S4 and results shown in Fig. S8 (a) and (b), respectively. It was observed that both isotherm models were well-fitted with the equilibrium desorption data of arsenic with a high coefficient of determination values (R^2) as summarized in Table S8. However, comparing the R^2 values of the Langmuir and Freundlich models, the Langmuir model conformed well with the desorption data of arsenic better than the Freundlich model demonstrating that arsenic ions recovery proceeded mainly through the chemical desorption process which involves the breakage of chemical bonds existing between the adsorbed arsenic ions and functional groups on the spent activated carbon. With respect to the Langmuir isotherm model, the maximum quantity of arsenic ions desorbed from the spent activated carbon was found to be 86.96 mg/g.

The kinetic desorption data of arsenic fitted to the pseudo-first-order and pseudo-second-order models are summarized in Text S5 and results displayed in Fig. S9 (a) and (b), respectively, and the kinetic parameters are summarized in Table S9. The kinetic desorption data of As is well described by both the pseudo-first-order and pseudo-second-order models. However, the pseudo-second-order kinetic model correlated well with the desorption data of arsenic with a higher R^2 of 0.9999 than the pseudo-first-order model revealing the possibility of chemical desorption as also suggested by the best-fitted Langmuir model. The calculated equilibrium desorption capacity value of 11.71 mg/g was close to the experimental value of 11.50 mg/g indicating the viability of the pseudo-second-order model to fit the experimental data of arsenic during its desorption from the spent activated carbon.

For the thermodynamic parameters evaluated as detailed in Text S6, the desorption process of arsenic ions was found to follow a spontaneous and feasible trend due to the negative values of ΔG° obtained for the temperature range (283.0–333.0 K) studied (Table S10). The decrease in the values of ΔG° with rising temperature indicated that higher temperatures facilitated the desorption of arsenic ions from the spent activated carbon. The positive value of ΔH° confirmed an endothermic process during arsenic ions recovery with physical desorption characteristics as the value of ΔH° is smaller than 40.0 kJ/mol (Khan et al., 2020). Also, the positive value of ΔS° suggested an upsurge in randomness between the desorbed arsenic ions in the liquid phase and spent activated carbon.

3.6. Comparison to literature

The related studies for As ions removal from aqueous systems were compiled to compare the uptake capacity of the hybrid granular activated carbon prepared from maize plant biomass. Table 3 shows the

Table 3
Comparison between adsorption capacities obtained for different adsorbent materials.

Adsorbent	Uptake capacity (mg/g)	Reference
Hybrid granular activated carbon	86.96	Present study
Ferrihydrite-modified biochar	18.38	(Tian et al., 2022)
Amaltash seed	1.42	(Giri et al., 2021)
Java plum seed	1.45	(Giri et al., 2021)
Activated hematite (Fe_2O_3) iron ore	14.96	(Memon et al., 2021)
Nano-porous carbon magnetic composite	6.69	(Joshi et al., 2019)
Fly ash/zeolite-graphene oxide	0.05	(Soni and Shukla, 2019)
Chitosan	8.00	(Kwok et al., 2018)
Nano-chitosan	13.00	(Kwok et al., 2018)
Potato peel and rice husk ash	0.03	(Bibi et al., 2017)
Mulberry wood	5.00	(Zama et al., 2017)

uptake capacity of various adsorbents applied for the decontamination of As ions from aquatic systems. It was found that among the complied studies, the hybrid granular activated carbon prepared from the maize plant residues shows higher sorption capacity than all the other adsorbents utilized in the previous studies. Therefore, the as-prepared activated carbon employed in this current study is more proficient for As ions removal and could be utilized as a promising adsorbent for the decontamination of other heavy metal ions from aquatic environments.

4. Conclusion

The current study investigated the desorption ability of arsenic species adsorbed on the activated carbon and the optimization of the independent factors influencing the proficient recovery of arsenic ions on the spent activated carbon using the central composite design of the response surface methodology. The study found that all the investigated independent desorption variables greatly influence the retrievability of the arsenic ions from the spent adsorbent. It was revealed that the successful desorption of arsenic species on the used activated carbon was favored at higher eluent concentration and desorption temperature, while keeping the pH of the solution at a lower value, especially in a more acidic medium.

The analysis of variance and residuals analysis demonstrated that the developed quadratic model was appropriate and accurate with a high R-squared of 0.9555 and an adequate precision of 21.31. Using the desirability function in the central composite design of the response surface methodology for the optimization of the independent factors as a function of desorption efficiency, the optimum experimental conditions attained after seeking 20 optimization solutions were solution pH of 2.0, eluent concentration of 0.1 M, and temperature of 26.6 ℃. At this optimum operating condition, the maximum arsenic ions desorbed from the spent activated carbon was 91 % with a desirability of 0.937. The validation of the quadratic model developed from the desorption ability of arsenic ions from the spent activated carbon was done by conducting laboratory confirmatory experiments, which yielded an optimum arsenic ions recovery efficiency of 96.75 %. The obtained optimum desorption efficiency from the laboratory confirmatory experiments was between the 95 % confidence prediction interval of 84–97 %. In comparison, there existed a good agreement between the confirmatory experimental and the predicted results with a standard error prediction of 2.74.

More so, the desorption isotherm and kinetic data of arsenic were well correlated with the Langmuir and the pseudo-second-order models, while the thermodynamics studies indicated that the desorption of the arsenic ions on the spent activated carbon was feasible, endothermic in nature, and spontaneous with upsurged randomness between the desorbed arsenic ions and spent activated carbon. The study therefore, concludes that the application of the central composite design of the response surface methodology led to the development of an accurate and valid quadratic model, which was utilized in predicting the response and optimization of the desorption parameters for effective recoverability of arsenic ions from the spent activated carbon for the purpose of reusability and proper disposal of the exhausted sorbent material.

CRediT authorship contribution statement

Jonas Bayuo: Writing – original draft, Visualization, Software, Methodology, Investigation, Funding acquisition, Formal analysis, Data curation, Conceptualization. **Mwemezi J. Rwiza:** Writing – review & editing, Validation, Supervision, Software, Resources, Methodology, Formal analysis, Data curation, Conceptualization. **Joon Weon Choi:** Writing – review & editing, Visualization, Validation, Supervision, Methodology, Conceptualization, Project administration. **Mika Sillanpää:** Writing – review & editing, Visualization, Validation, Methodology, Data curation, Conceptualization. **Kelvin Mark Mtei:** Writing – review & editing, Visualization, Validation, Supervision, Resources, Project administration, Methodology, Conceptualization.

Declaration of Competing Interest

The authors declare that they have no known competing financial interests or personal relationships that could have appeared to influence the work reported in this paper.

Data availability

Data will be made available on request.

Acknowledgements

This work was funded by the Partnership for Applied Sciences, Engineering, and Technology-Regional Scholarship and Innovation Fund (PASET-Rsif) and the Carnegie Corporation of New York (CCNY) with grant number P165581. In addition, this work was supported by the Korea Forest Service (Korea Forestry Promotion Institute) through the R&D Program for Forest Science Technology (Project No. 2023483B10–2325-AA01).

Appendix A. Supporting information

Supplementary data associated with this article can be found in the online version at doi:10.1016/j.ecoenv.2024.116550.

References

Afolabi, F.O., Musonge, P., Bakare, B.F., 2021. Bio-sorption of a bi-solute system of copper and lead ions onto banana peels: characterization and optimization. J. Environ. Health Sci. Eng. *19* (1), 613–624. https://doi.org/10.1007/s40201-021-00632-x.

Afraz, V., Younesi, H., Bolandi, M., Hadiani, M.R., 2020. Optimization of lead and cadmium biosorption by Lactobacillus acidophilus using response surface methodology. Biocatal. Agric. Biotechnol. *29* (January), 101828 https://doi.org/10.1016/j.bcab.2020.-101828.

Alimohammady, M., Jahangiri, M., Kiani, F., Tahermansouri, H., 2017. Highly efficient simultaneous adsorption of Cd(II), Hg(II) and As(III) ions from aqueous solutions by modification of graphene oxide with 3-aminopyrazole: central composite design optimization. N. J. Chem. *41* (17), 8905–8919. https://doi.org/10.1039/c7-nj01450c.

Bai, M.T., Venkateswarlu, P., 2019. Optimization studies for lead biosorption on Sargassum tenerrimum (Brown Algae) using experimental design: response surface methodology. Mater. Today.: Proc. *18*, 4290–4298. https://doi.org/10.1016/j.matpr.2019.07.387.

Bangaraiah, P., Peele, K.A., Venkateswarulu, T.C., 2021. Removal of lead from aqueous solution using chemically modified green algae as biosorbent: optimization and kinetics study. Int. J. Environ. Sci. Technol. *18* (2), 317–326. https://doi.org/10.1007/s13762-020-02810-0.

Bayuo, J., Abukari, M.A., Pelig-Ba, K.B., 2020. Desorption of chromium (VI) and lead (II) ions and regeneration of the exhausted adsorbent. Appl. Water Sci. *10* (7), 1–6. https://doi.org/10.1007/s13201-020-01250-y.

Bayuo, J., Rwiza, M.J., Mtei, K., 2022. Response surface optimization and modeling in heavy metal removal from wastewater—a critical review. Environ. Monit. Assess. *194* (5), 1–34. https://doi.org/10.1007/s10661-022-09994-7.

Bayuo, J., Rwiza, M.J., Mtei, K.M., 2023a. Adsorption and desorption ability of divalent mercury from an interactive bicomponent sorption system using hybrid granular activated carbon. Environ. Monit. Assess. *195* (935), 1–17 https://doi.org/10.-1007/s10661-023-11540-y.

Bayuo, J., Rwiza, M.J., Mtei, K.M., 2023b. Non-competitive and competitive detoxification of As(III) ions from single and binary biosorption systems and biosorbent regeneration. Biomass-.-. Convers. Biorefinery 1–28. https://doi.org/10.1007/s13399-022-03734-0.

Bhateria, R., Dhaka, R., 2019. Optimization and statistical modelling of cadmium biosorption process in aqueous medium by Aspergillus niger using response surface methodology and principal component analysis (https://doi.-org/). Ecol. Eng. *135* (May), 127–138. https://doi.org/10.1016/j.ecoleng.2019.05.010.

Bi, X., Zeng, C., Westerhoff, P., 2020. Adsorption of arsenic ions transforms surface reactivity of engineered cerium oxide nanoparticles. Environ. Sci. Technol. *54* (15), 9437–9444. https://doi.org/10.1021/acs.est.0c02781.

Biswas, S., Meikap, B.C., Sen, T.K., 2019. Adsorptive removal of aqueous phase copper (Cu2+) and nickel (Ni2+) metal ions by synthesized biochar–biopolymeric hybrid adsorbents and process optimization by response surface methodology (RSM). Water, Air, Soil Pollut. *230* (8) https://doi.org/10.1007/s11270-019-4258-y.

Biswas, S., Sharma, S., Mukherjee, S., Meikap, B.C., Sen, T.K., 2020. Process modelling and optimization of a novel Semifluidized bed adsorption column operation for

aqueous phase divalent heavy metal ions removal. J. Water Process Eng. *37* (April), 101406 https://doi.org/10.1016/j.jwpe.2020.101406.
Brahmi, L., Kaouah, F., Boumaza, S., Trari, M., 2019. Response surface methodology for the optimization of acid dye adsorption onto activated carbon prepared from wild date stones. Appl. Water Sci. *9* (8), 1–13. https://doi.org/10.1007/s13201-019-1053-2.
Chen, L., Xiong, Q., Li, S., Li, H., Chen, F., Zhao, S., Ye, F., Hou, H., Zhou, M., 2020. The experimental optimization and comprehensive environmental risk assessment of heavy metals during the enhancement of sewage sludge dewaterability with ethanol and Fe(III)-rice husk. J. Environ. Manag. *273* (July), 111122 https://doi.org/10.1016/j.-jenvman.2020.111122.
Cheng, J., Gao, J., Zhang, J., Yuan, W., Yan, S., Zhou, J., Zhao, J., Feng, S., 2021. Optimization of hexavalent chromium biosorption by shewanella putrefaciens using the box-Behnken design. Water, Air, Soil Pollut. *232* (3), 1–14 https://doi.org/10.-1007/s11270-020-04947-7.
Ciopec, M., Biliuta, G., Negrea, A., Duțeanu, N., Coseri, S., Negrea, P., Ghangrekar, M., 2021. Testing of chemically activated cellulose fibers as adsorbents for treatment of arsenic contaminated water. Materials *14* (13), 1–20. https://doi.org/10.3390/ma14133731.
Corral-Bobadilla, M., Lostado-Lorza, R., Somovilla-Gómez, F., Escribano-García, R., 2021. Effective use of activated carbon from olive stone waste in the biosorption removal of Fe(III) ions from aqueous solutions. J. Clean. Prod. *294* https://doi.org/10.1016/j.-jclepro.2021.126332.
Deng, M., Wu, X., Zhu, A., Zhang, Q., Liu, Q., 2019. Well-dispersed TiO 2 nanoparticles anchored on Fe 3 O 4 magnetic nanosheets for efficient arsenic removal. J. Environ. Manag. *237*, 63–74. https://doi.org/10.1016/j.jenvman.2019.02.037.
Dulla, J.B., Tamana, M.R., Boddu, S., Pulipati, K., Srirama, K., 2020. Biosorption of copper(II) onto spent biomass of Gelidiella acerosa (brown marine algae): optimization and kinetic studies. Appl. Water Sci. *10* (2), 1–10. https://doi.org/10.1007/s13201-019-1125-3.
El-Ahmady El-Naggar, N., Rabei, N.H., El-Malkey, S.E., 2020. Eco-friendly approach for biosorption of Pb2+ and carcinogenic Congo red dye from binary solution onto sustainable Ulva lactuca biomass. Sci. Rep. *10* (1), 2052. https://doi.org/10.1038/s41598-020-73031-1.
Ezeonuegbu, B.A., Machido, D.A., Whong, C.M.Z., Japhet, W.S., Alexiou, A., Elazab, S.T., Qusty, N., Yaro, C.A., Batiha, G.E.S., 2021. Agricultural waste of sugarcane bagasse as efficient adsorbent for lead and nickel removal from untreated wastewater: biosorption, equilibrium isotherms, kinetics and desorption studies. Biotechnol. Rep. *30*, 1–10. https://doi.org/10.1016/j.btre.2021.e00614.
Fawzy, M.A., 2020. Biosorption of copper ions from aqueous solution by Codium vermilara: optimization, kinetic, isotherm and thermodynamic studies. Adv. Powder Technol. *31* (9), 3724–3735. https://doi.org/10.1016/j.apt.2020.07.014.
Fawzy, M.A., Darwish, H., Alharthi, S., Al-Zaban, M.I., Noureldeen, A., Hassan, S.H.A., 2022. Process optimization and modeling of Cd2+ biosorption onto the free and immobilized Turbinaria ornata using Box–Behnken experimental design. Sci. Rep. *12* (1), 1–18. https://doi.org/10.1038/s41598-022-07288-z.
Gan, C., Liu, M., Lu, J., Yang, J., 2020. Adsorption and desorption characteristics of vanadium (V) on silica. Water, Air, Soil Pollut. *231* (1), 1–11 https://doi.org/10.-1007/s11270-019-4377-5.
Ghangale, S.S., Bholay, A., Saler, R., 2019. Biosorption and desorption of heavy metal lead (ii) from aqueous solution using Vitis vinifera leaves as an agro waste biomass. J. Inf. Comput. Sci. *12* (6), 62–73.
Gilcreas, F.W. (1967). Future of standard methods for the examination of water and wastewater. In *Health laboratory science* (23rd ed., Vol. 4, Issue 3). American Public Health Association, American Water Works Association, and Water Environment Federation. http://www.ajph.-org/cgi/doi/10.2105/AJPH.51.6.940-a.
Gomravi, Y., Karimi, A., Azimi, H., 2021. Adsorption of heavy metal ions via apple waste low-cost adsorbent: characterization and performance. Korean J. Chem. Eng. *38* (9), 1843–1858. https://doi.org/10.1007/s11814-021-0802-8.
Hadiani, M.R., Khosravi-Darani, K., Rahimifard, N., 2019. Optimization of As (III) and As (V) removal by Saccharomyces cerevisiae biomass for biosorption of critical levels in the food and water resources. J. Environ. Chem. Eng. *7* (2), 1–9. https://doi.org/10.1016/j.jece.2019.102949.
Hamza, M.F., Alotaibi, S.H., Wei, Y., Mashaal, N.M., 2022. High-performance hydrogel based on modified chitosan for removal of heavy metal ions in borehole: a case study from the bahariya oasis. Egypt. *Catal.* *12* (7), 1–21. https://doi.org/10.3390/catal-12070721.
Hannachi, Y., Hafidh, A., 2020. Biosorption potential of Sargassum muticum algal biomass for methylene blue and lead removal from aqueous medium. Int. J. Environ. Sci. Technol. *17* (9), 3875–3890. https://doi.org/10.1007/s13762-020-02742-9.
Hua, M., Zhang, S., Pan, B., Zhang, W., Lv, L., Zhang, Q., 2012. Heavy metal removal from water/wastewater by nanosized metal oxides: a review. J. Hazard. Mater. *211–212*, 317–331. https://doi.org/10.1016/j.jhazmat.2011.10.016.
Jadidi, M., Etesami, N., Nasr Esfahany, M., 2017. Adsorption and desorption process of chromium ions using magnetic iron oxide nanoparticles and its relevant mechanism. Iran. J. Chem. Eng. (IJChE) *14* (3), 31–40.
John, D.B., King, P., Prasanna Kumar, Y., 2019. Optimization of Cu (II) biosorption onto sea urchin test using response surface methodology and artificial neural networks. Int. J. Environ. Sci. Technol. *16* (4), 1885–1896. https://doi.org/10.1007/s13762-018-1747-2.
Joseph, L., Jun, B.M., Flora, J.R.V., Park, C.M., Yoon, Y., 2019. Removal of heavy metals from water sources in the developing world using low-cost materials: a review. Chemosphere *229*, 142–159. https://doi.org/10.1016/j.chemosphere.2019.04.198.
Karapinar, H.S., Kilicel, F., Ozel, F., Sarilmaz, A., 2021. Fast and effective removal of Pb (II), Cu(II) and Ni(II) ions from aqueous solutions with TiO2 nanofibers: synthesis, adsorption-desorption process and kinetic studies. Int. J. Environ. Anal. Chem. *00* (00), 1–21. https://doi.org/10.1080/03067319.2021.1931162.
Khan, Z.H., Gao, M., Qiu, W., Qaswar, M., Islam, M.S., Song, Z., 2020. The sorbed mechanisms of engineering magnetic biochar composites on arsenic in aqueous solution. Environ. Sci. Pollut. Res. *27* (33), 41361–41371 https://doi.org/10.-1007/s11356-020-10082-x.
Khoshraftar, Z., Masoumi, H., Ghaemi, A., 2023. Experimental, response surface methodology (RSM) and mass transfer modeling of heavy metals elimination using dolomite powder as an economical adsorbent. Case Stud. Chem. Environ. Eng. *7* (February), 100329 https://doi.org/10.1016/j.cscee.2023.100329.
Kocadagistan, B., Oksuz, K., 2022. Pb (II) recovery by modified tuffite: adsorption, desorption, and kinetic study. Adsorpt. Sci. Technol. *2022*, 1–17. https://doi.org/10.1155/2022/7195777.
Kołodyńska, D., Krukowska, J., Thomas, P., 2017. Comparison of sorption and desorption studies of heavy metal ions from biochar and commercial active carbon. Chem. Eng. J. *307*, 353–363. https://doi.org/10.1016/j.cej.2016.08.088.
Kushwaha, D., Dutta, S., 2017. Experiment, modeling and optimization of liquid phase adsorption of Cu(II) using dried and carbonized biomass of Lyngbya majuscula. Appl. Water Sci. *7* (2), 935–949. https://doi.org/10.1007/s13201-015-0304-0.
Kusrini, E., Usman, A., Sani, F.A., Wilson, L.D., Abdullah, M.A.A., 2019. Simultaneous adsorption of lanthanum and yttrium from aqueous solution by durian rind biosorbent. Environ. Monit. Assess. *191* (8), 488.1–488.8 https://doi.org/10.-1007/s10661-019-7634-6.
Li, H., Li, X., Chen, Y., Long, J., Zhang, G., Xiao, T., Zhang, P., Li, C., Zhuang, L., Huang, W., 2018. Removal and recovery of thallium from aqueous solutions via a magnetite-mediated reversible adsorption-desorption process. J. Clean. Prod. *199*, 705–715. https://doi.org/10.1016/j.jclepro.2018.07.178.
Liang, C. li, Shen, J. li, 2022. Removal of yttrium from rare-earth wastewater by Serratia marcescens: biosorption optimization and mechanisms studies. Sci. Rep. *12* (1), 1–14. https://doi.org/10.1038/s41598-022-08542-0.
Liu, L., Lin, X., Luo, L., Yang, J., Luo, J., Liao, X., Cheng, H., 2021. Biosorption of copper ions through microalgae from piggery digestate: optimization, kinetic, isotherm and mechanism. J. Clean. Prod. *319* (March)), 128724 https://doi.org/10.1016/j.-jclepro.2021.128724.
Liu, X., Han, B., Su, C. li, Han, Q., Chen, K. jie, Chen, Z. qiong, 2019. Optimization and mechanisms of biosorption process of Zn(II) on rape straw powders in aqueous solution. Environ. Sci. Pollut. Res. *26* (31), 32151–32164 https://doi.org/10.-1007/s11356-019-06342-0.
Lu, M., Zhang, Y., Zhou, Y., Su, Z., Liu, B., Li, G., Jiang, T., 2019. Adsorption-desorption characteristics and mechanisms of Pb(II) on natural vanadium, titanium-bearing magnetite-humic acid magnetic adsorbent. Powder Technol. *344*, 947–958 https://doi.org/10.-1016/j.powtec.2018.12.081.
Lyonga, F.N., Hong, S.H., Cho, E.J., Kang, J.K., Lee, C.G., Park, S.J., 2021. As(III) adsorption onto Fe-impregnated food waste biochar: experimental investigation, modeling, and optimization using response surface methodology. Environ. Geochem. Health *43* (9), 3303–3321. https://doi.org/10.1007/s10653-020-00739-4.
Mahmood, T., Ali, R., Naeem, A., Hamayun, M., Aslam, M., 2017. Potential of used Camellia sinensis leaves as precursor for activated carbon preparation by chemical activation with H3PO4; optimization using response surface methodology. Process Saf. Environ. Prot. *109*, 548–563. https://doi.org/10.1016/j.psep.2017.04.024.
Mladin, G., Ciopec, M., Negrea, A., Duteanu, N., Negrea, P., Ianasi, P., Ianași, C., 2022. Silica- iron oxide nanocomposite enhanced with porogen agent used for arsenic removal. Materials *15* (15), 1–23. https://doi.org/10.3390/ma15155366.
Mondal, N.K., Basu, S., Das, B., 2019. Decontamination and optimization study of hexavalent chromium on modified chicken feather using response surface methodology. Appl. Water Sci. *9* (3), 1–15. https://doi.org/10.1007/s13201-019-0930-z.
Mushtaq, M., Arshad, N., Hameed, M., Munir, A., Javed, G.A., Rehman, A., 2023. Lead biosorption efficiency of Levilactobacillus brevis MZ384011 and Levilactobacillus brevis MW362779: A response surface based approach. Saudi J. Biol. Sci. *30* (2), 103547 https://doi.org/10.1016/j.sjbs.2022.103547.
Parmar, P., Shukla, A., Goswami, D., Patel, B., Saraf, M., 2020. Optimization of cadmium and lead biosorption onto marine Vibrio alginolyticus PBR1 employing a Box-Behnken design. Chem. Eng. J. Adv. *4* (October) https://doi.org/10.1016/j.-ceja.2020.100043.
Priyadarshanee, M., Das, S., 2021. Biosorption and removal of toxic heavy metals by metal tolerating bacteria for bioremediation of metal contamination: a comprehensive review. J. Environ. Chem. Eng. *9* (1), 104686 https://doi.org/10.1016/j.-jece.2020.104686.
Sadhukhan, B., Mondal, N.K., Chattoraj, S., 2016. Optimisation using central composite design (CCD) and the desirability function for sorption of methylene blue from aqueous solution onto Lemna major. Karbala Int. J. Mod. Sci. *2* (3), 145–155. https://doi.org/10.1016/j.kijoms.2016.03.005.
Saleh, S., Mohammadnejad, S., Khorgooei, H., Otadi, M., 2021. Photooxidation/adsorption of arsenic (III) in aqueous solution over bentonite/ chitosan/TiO2 heterostructured catalyst. Chemosphere *280* (April), 130583. https://doi.org/10.1016/j.chemosphere.2021.130583.
Staroń, P., Płecka, A., Chwastowski, J., 2021. Lead sorption by chrysanthemum indicum: equilibrium, kinetic, and desorption studies. Water, Air, Soil Pollut. *232* (1), 1–14. https://doi.org/10.1007/s11270-020-04956-6.
Taşdemir, R., Yiğitarslan, S., Erzengin, S.G., 2021. Optimization of lead (II) adsorption onto cross-linked polycarboxylate-based adsorbent by response surface methodology. Arab. J. Sci. Eng. *46* (7), 6287–6301. https://doi.org/10.1007/-s13369-020-05029-w.

Tokay, B., Akpınar, I., 2021. A comparative study of heavy metals removal using agricultural waste biosorbents. Bioresour. Technol. Rep. *15*, 1–9. https://doi.org/10.1016/j.-biteb.2021.100719.

Touihri, M., Gouveia, S., Guesmi, F., Hannachi, C., Hamrouni, B., Cameselle, C., 2021. Low-cost biosorbents from pines wastes for heavy metals removal from wastewater: adsorption/desorption studies. Desalin. Water Treat. *225*, 430–442. https://doi.org/10.5004/dwt.2021.27145.

Ünügül, T., Nigiz, F.U., 2022. Optimization of sodium alginate-graphene nanoplate-kaolin bio-composite adsorbents in heavy metal adsorption by response surface methodology (RSM). Arab. J. Sci. Eng. *47* (5), 6001–6012. https://doi.org/10.1007/s13369-021-05905-z.

Vakili, M., Deng, S., Cagnetta, G., Wang, W., Meng, P., Liu, D., Yu, G., 2019. Regeneration of chitosan-based adsorbents used in heavy metal adsorption: a review. Sep. Purif. Technol. *224* (May), 373–387. https://doi.org/10.1016/j.seppur.2019.05.040.

Xie, S., Wen, Z., Zhan, H., Jin, M., 2018. An experimental study on the adsorption and desorption of Cu(II) in Silty clay. Geofluids *2018*, 1–13. https://doi.org/10.1155/-2018/3610921.

Yuan, W., Cheng, J., Huang, H., Xiong, S., Gao, J., Zhang, J., Feng, S., 2019. Optimization of cadmium biosorption by Shewanella putrefaciens using a Box-Behnken design. Ecotoxicol. Environ. Saf. *175* (January), 138–147. https://doi.org/10.1016/j.-ecoenv.2019.03.057.

Zhang, J., Hu, X., Zhang, K., Xue, Y., 2019. Desorption of calcium-rich crayfish shell biochar for the removal of lead from aqueous solutions. J. Colloid Interface Sci. *554*, 417–423. https://doi.org/10.1016/j.jcis.2019.06.096.

Zou, C., Jiang, W., Liang, J., Guan, Y., Sun, X., 2019. Desorption regeneration performance of magnetic bentonite after Pb(II) adsorbed. ChemistrySelect *4* (4), 1306–1315. https://doi.org/10.1002/slct.201802613.